metals

MDPI

Article

Effect of Deep Cryogenic Treatment on the Microstructure and the Corrosion Resistance of AZ61 Magnesium Alloy Welded Joint

Xiaoyuan Gong *, Zhisheng Wu and Fei Zhao

Materials Science and Engineering academy, Taiyuan University of Science and Technology, Taiyuan 030024, China; liye@tyust.edu.cn (Z.W.); jliu43@jmc.com.cn (F.Z.)

* Correspondence: ljqsky@126.com; Tel.: +86-182-3411-6948

Academic Editor: Daolun Chen

Received: 28 March 2017; Accepted: 12 May 2017; Published: 17 May 2017

Abstract: The effect of deep cryogenic treatment on the microstructure and corrosion resistance of an AZ61 magnesium alloy metal inert-gas (MIG) welded joint was investigated. The welded joints were deep-cryogenically treated using different parameters, and were analyzed by metallographic observations, X-ray diffraction, microhardness, and NaCl immersion test. The results show that the treatment changes the microstructure of the entire joint by causing grain refinement and increase in the β-phase. The crystal structure, chemical composition, and electrode potentials are different for the α and the β-phases. Therefore, any change in content, status, and distribution of the β phase has important implications on the corrosion resistance of the samples. With an increase in the holding time, the microhardness value of the whole joint increases, and the difference between the three regions of the joint decreases. The results of the NaCl immersion test show that there is an improvement in the corrosion resistance of the treated joints. Compared with the untreated samples, the corrosion potential of the samples treated by deep cryogenic treatment for 4 h at −180 °C is about 0.017 V higher, and the corrosion current density decreased by one order of magnitude (from about 2.769×10^{-5} A·cm^{-2} to 1.578×10^{-6} A·cm^{-2}).

Keywords: welded joints; deep cryogenic treatment; microstructure; corrosion resistance

1. Introduction

Cryogenic processing refers to placing a material in a specific and controllable ultra-low-temperature environment to change its microstructure, so as to improve its material properties [1,2].

Owing to the features such as low density, high specific strength, good recovery, etc., the structural magnesium alloys have extremely important industrial applications. The high thermal conductivity of the magnesium alloys demands the use of a high-powered welding heat source during the welding process. This also leads to different microstructural characteristics in the three regions of the joints. In particular, the heat affected zone (HAZ) is prone to overheating, grain growth, and segregation. These changes affect the mechanical properties and the corrosion resistance of the joints. The effect of deep cryogenic treatment on the microstructure and the corrosion resistance of the AZ61 magnesium alloy metal inert-gas (MIG) welded joint was studied in this work.

2. Materials and Processes

2.1. Test Materials

The dimensions of the AZ61 magnesium alloy sheets were 200 mm × 150 mm × 7 mm, and the chemical composition of the welding wire was the same as the base metal. Diameter of the welding wire was 1.6 mm. The chemical compositions of the base metal and the wire are shown in Table 1.

Table 1. Chemical composition of MB5 magnesium alloy.

Al	Mn	Zn	Cu	Si	Ni	Fe	Impurities	Mg
5.8–7.2	0.15 min	0.4–1.5	0.05 max	0.30 max	0.005 max	0.005 max	0.30 max	other

2.2. Welding Process

A direct-current (DC) MIG welding machine (Fronius Company, Pettenbach, Austria) was used for multi-layer welding. The AZ61 magnesium alloy sheets take a single 45° groove, do not keep a blunt edge, and leave no root gap, as shown in Figure 1.

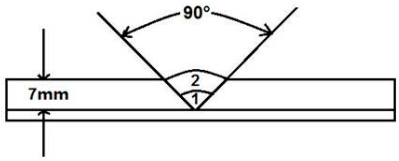

Figure 1. Groove schematic.

The welded joint was prepared using the Fuis TPS5000 digitized pulsed MIG welder (Fronius Company, Pettenbach, Austria), which uses an all-digital microprocessor-controlled inverter power supply that utilizes advanced cold metal transfer (CMT) technology. This technology can achieve the digital control mode of short-arc and wire feed monitoring. The process parameters are listed in Table 2.

Table 2. Welding parameters.

Process Parameters	Wire Feed Speed (m/min)	Current (A)	Voltage (V)	Welding Speed (m/min)
The first pass	9.2	123	9.6	0.7
Second pass	13	165	11	0.35
Swing settings	Pendulum length: 3.5 mm, swing: 4 mm, jagged side swing			
Nozzle diameter	15 mm			
Argon flow	14 L/min			
Wire diameter	1.6 mm			

2.3. Cryogenic Treatment Process

Joints of sizes 16 mm × 10 mm × 10 mm were cut along the weld direction, and then the samples were placed in the deep cryogenic treatment box. The samples were cooled from 20 °C to −180 °C at a rate of 6 °C/min, held at −180 °C for a certain time, and then slowly warmed to room temperature (25 °C). The cryogenic treatment temperature was −180 °C, the holding times were 4 h, 6 h, and 8 h. The samples were polished with 200#, 600#, 1000#, and 1500# grit sandpapers, and finally with 0.1 mm diamond paste to get a mirror-like surface. They were rinsed in distilled water and alcohol before etching in picric acid. The samples were prepared for optical and scanning electron microscopy.

The microstructures of the samples were observed using the Aokang XJ-300 metallographic microscope (Nanjing Aokang Analytical Instruments Co., Ltd., Nanjing, China) and the Hitachi high-tech SU3500 scanning electron microscope (Hitachi Limited, Hitachi, Japan).

NaCl immersion and electrochemical corrosion tests were conducted using 3.5% NaCl solution as the electrolyte.

3. Results and Analysis

3.1. Microstructure

The solubility of aluminum in magnesium decreases and the β-phase precipitates along the dislocation lines and grain boundaries after the deep cryogenic treatment. This increases gradually

during the treatment and does not disappear during the subsequent temperature recovery process. Internal stresses and related strains are created in the material during the deep cryogenic treatment, which cause proliferation of the dislocations and precipitation of the β-phase and the sub crystals. These microstructural changes cause grain refinement. The extremely low temperatures and low kinetic energies of the atoms lead to a difficulty in proliferation, which suppresses the growth of the β-phase. This leads to the formation of a continuous network of the β-phase with a very small grain size [3].

The microstructures of the samples before and after the deep cryogenic treatment are observed and analyzed. The black particles seen in Figure 2 are the β-phase particles. Due to the large heat input during the welding process and rapid cooling after the welding process, the structure of the weld metal is a product of non-equilibrium crystals. Therefore, the β-phase content in the weld zone is higher than that in the base metal [4]. The weld zone has the finest grain sizes and more grain boundary area than the other zones. The β-phase of the weld zone increased significantly when the deep cryogenic treatment time was 4 h, as shown in Figure 2b. With the decrease in the cryogenic treatment temperature, there was an increase in the base material area of the joint, especially in the HAZ, where the sub grain formation was easier. The precipitation of the β-phase in the base metal and the HAZ increased significantly, and the precipitation of β-phase did not continue indefinitely, but gradually stabilized [5]. As compared with the other parameters, the difference between the contents of the β-phase in the three regions of the weld joint was minimum, and the β-phase was distributed in a continuous network status when the deep cryogenic treatment time was 8 h. This can be observed in Figure 2c,d.

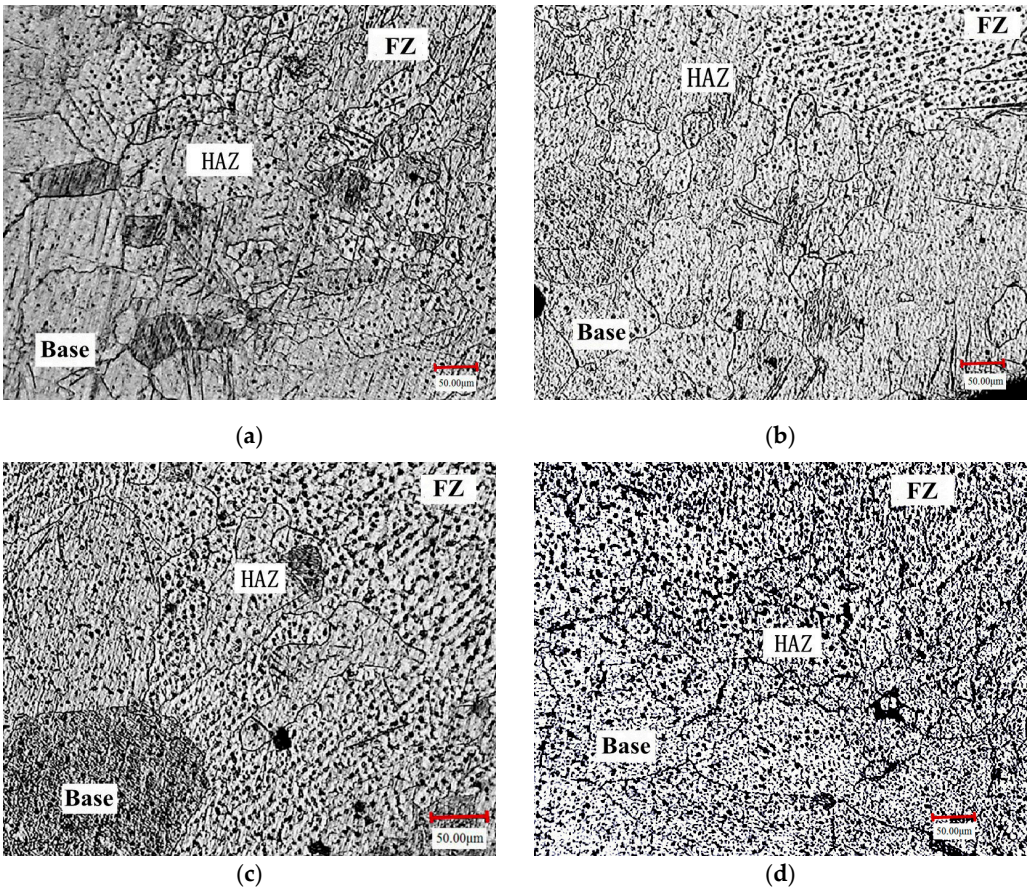

Figure 2. Organizational change of AZ61 magnesium alloy welded joints in different deep cryogenic treatment holding time (−180 °C): (**a**) Before cryogenic treatment; (**b**) After cryogenic treatment (−180 °C, 4 h); (**c**) After cryogenic treatment (−180 °C, 6 h); (**d**) After cryogenic treatment (−180 °C, 8 h). HAZ: heat-affected zone. FZ: fuse zone.

3.2. Micro-Hardness

The welding process leads to the formation of coarse grains and a negative tissue zone in the HAZ. Therefore, the HAZ has the minimum hardness value in the joint, followed by the base metal, and then by the weld zone, which has the maximum hardness value. With the deep cryogenic treatment, the difference in the β-phase content in the joints was gradually reduced. The micro-hardness of the HAZ shows the sharpest increase after treatment, as shown in Figure 3. With an increase in the deep cryogenic treatment time, the micro-hardness curve of the three regions of the joint gradually softens.

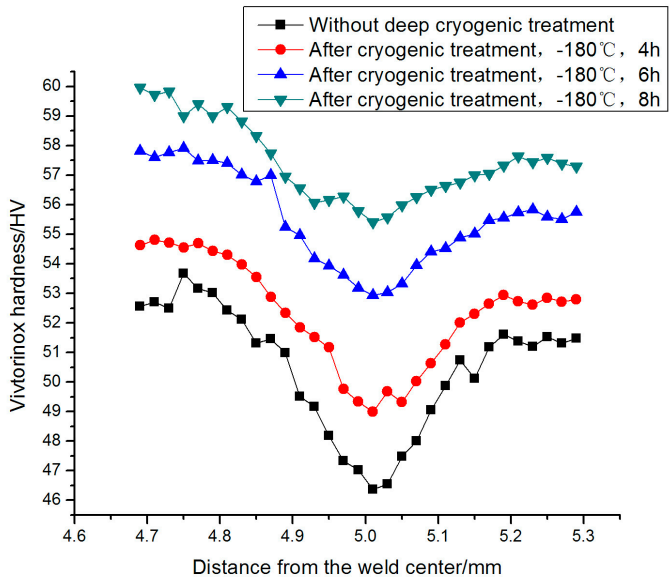

Figure 3. Hardness curve at different deep cryogenic treatment temperatures.

The change in the internal stress plays an important role in improving the overall micro-hardness of the sample. The first hardness peak appears when the deep cryogenic treatment time is short (4 h). The internal stress causes a change that lasts for a shorter duration, while the precipitation of the β-phase causes a change that lasts longer. With prolonged deep cryogenic treatment, there is an increase in the number of β particles playing an important role in increasing the micro-hardness. The second hardness peak appears (during the process of 6 h → 8 h) when the precipitation of β-phase is completed. The precipitation of the β-phase is limited, just like the precipitation of sub-grains. So, the hardness value of the joint does not continuously increase with the increase in the deep cryogenic treatment time.

3.3. Analysis of X-ray Diffraction Pattern

The phase composition of the weld joint was analyzed by X-ray diffraction (XRD) before and after the deep cryogenic treatment. As seen in the XRD patterns in Figure 4, the deep cryogenic treatment does not change the phase composition of the joint. A part of the characteristic peak value of the crystal plane is changed, indicating that when there was a grain refinement after the deep cryogenic treatment, a part of the grains have a preferred orientation, grain rotation, or texture. There is an increase in the diffraction peak of the β-phase in the treated samples compared with the untreated samples; the treated samples precipitate more β-phase.

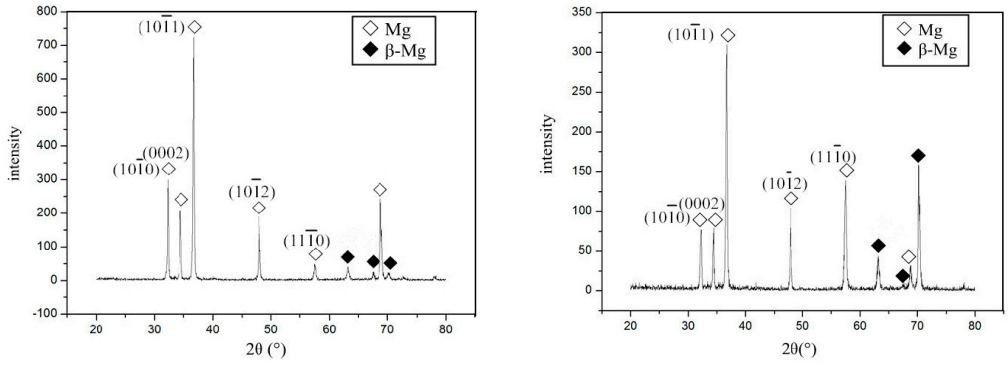

(**a**) Before cryogenic treatment (**b**) After cryogenic treatment, −180 °C, 8 h

Figure 4. XRD analysis of AZ61 welded joint (**a**) before and (**b**) after cryogenic treatment.

4. Corrosion Studies

NaCl Immersion Test

Cao et al. [6] considers that the β-phase in the Mg-Al-based alloy has two functions, acting as the cathode and the corrosion barrier. The α-phase also affects the corrosion rate of the alloy. The refinement of the α-phase can make the β-phase precipitate around the α-phase, forming a continuous network and thus improving the corrosion resistance of the magnesium alloy.

Mónica et al. [7] found that with the deep cryogenic treatment, a continuous network of the β-phase is distributed in the α-matrix, and that the organization of the α-matrix can be enhanced by the refined β-phase. The β-phase also plays an important role in blocking the α-phase that is peeled off from the surface. The deep cryogenic treatment changes the morphology and the distribution of the β-phase in the material, which increases the corrosion resistance of the alloy [7–9]. The β-phase is much harder than the α-phase, and its electrode potential is higher than that of the α-phase. The β-phase also possesses good chemical inertia. When the content of the β-phase is lower, the α-phase can be easily corroded. On the contrary, the increase in the β-phase content increases the source of pitting corrosion. Nevertheless, the high potential of the β-phase is good for corrosion resistance. In general, the β-phase plays an active role in providing corrosion resistance to the joints [10].

Figure 5 shows the SEM morphology of the samples without the deep cryogenic treatment that were immersed in the NaCl solution for 10 h. The degree of damage on the base metal and the HAZ is more serious than that on the weld zone. This is because of the lesser content of the β-phase in these two regions. The β-phase in the weld joint is a continuously distributed network that blocks the further expansion of corrosion. This is consistent with the previous analysis.

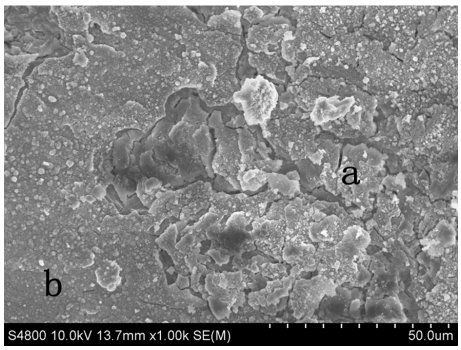

Figure 5. SEM images of the joint samples without cryogenic treatment immersed in NaCl solution after 10 h: **a**—Base metal and heat affected zone; **b**—the weld zone.

According to the previous analysis, all three regions of the joint have the same source of corrosion, but different corrosion resistances. The HAZ has the least corrosion resistance. The following experiments were performed in order to study the effect of cryogenic treatment on the corrosion resistance of the magnesium alloy welded joint.

Figure 6 shows the samples (HAZ) after different deep cryogenic treatment times that were immersed in NaCl solution for 20 h. With the decrease in deep cryogenic treatment time, the degree of corrosion damage on the sample surface increases, and the highest number of pits appear on the surface of the α-phase. The area and the number of the etch pits increase until the surface of the sample is almost destroyed, leaving a relatively corrosion-resistant β-phase. When the cryogenic treatment time is 8 h, there are some pits with a white inlay (the white material is the corrosion product), distributed randomly on the surface of the α-phase. The maximum diameter of the pits is about 15.33 μm. When the deep cryogenic treatment time is 6 h, tiny cracks appear around the pits that gradually extend to the surroundings, and the surface of the samples gradually loses its metallic luster. The surface of the samples is corroded when the deep cryogenic treatment time is 6 h. Further expansion of the cracks can be seen from Figure 6; the surface of the metal is partially stripped, and is covered with a portion of the corrosion product. However, in the samples without the cryogenic treatment, a part of the surface is covered with the white corrosion product, and the metal strip on the surface of the samples gradually deteriorates. A series of chemical reactions that occur during the immersion process and the relatively loose corrosion products lead to an expansion of the sample surface, causing a more serious damage to the sample surface. As shown in Figure 6a–c, the cracks originate in the α-phase and expand outward gradually with the decrease of the deep cryogenic treatment time. The degree of corrosion damage to the β-phase is relatively light.

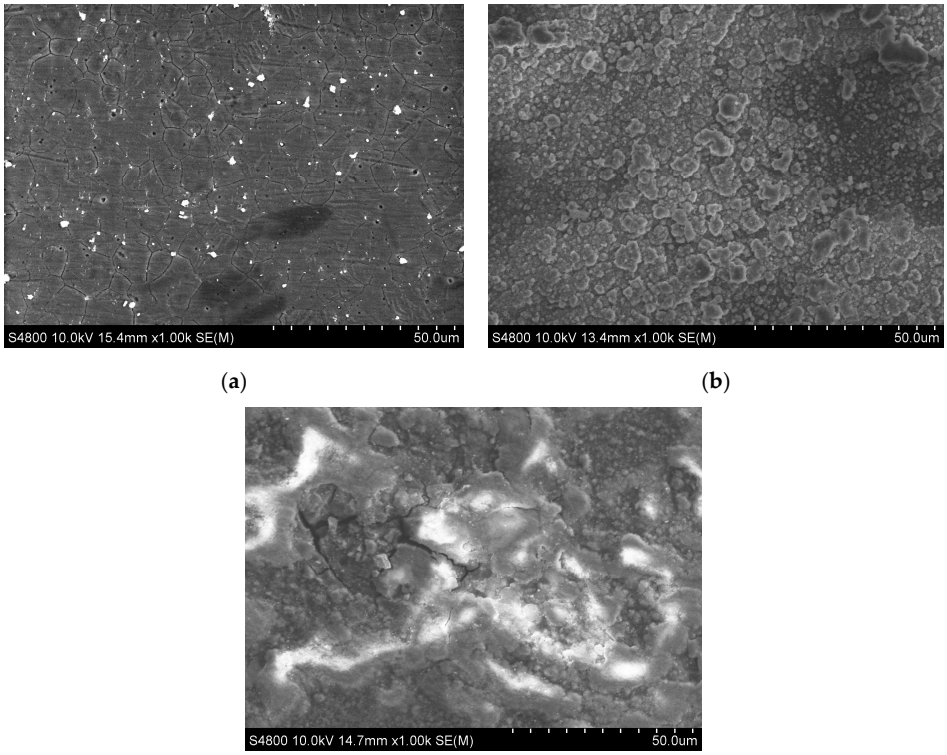

Figure 6. SEM images of the samples with different cryogenic processing parameters immersed in NaCl solution after 20 h; (**a**) After cryogenic treatment, −180 °C, 8 h; (**b**) After cryogenic treatment, −180 °C, 6 h; (**c**) After cryogenic treatment, −180 °C, 4 h.

The polarization curve of the samples with different deep cryogenic treatment times is shown in Figure 7. With an increase in the deep cryogenic treatment time, a gradual negative shift in the corrosion potential of the samples and a gradual decrease in the corrosion current are observed. As the corrosion rate of the samples decreases, the driving force of the cathodic reaction increases, leading to a negative shift in the corrosion potential. The cathodic reaction rate decreases with an increase in the deep cryogenic treatment time. As compared with the sample without the cryogenic treatment, the ones treated for 8 h at −180 °C show a decrease of about 0.017 V in the corrosion potential and a decrease in the corrosion current density by one order of magnitude (from 2.769×10^{-5} A·cm^{-2} to 1.578×10^{-6} A·cm^{-2}). The corrosion resistance is the best when these process parameters are used.

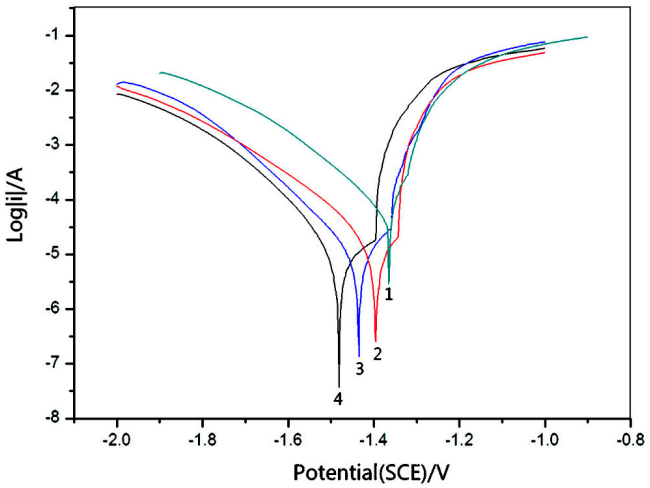

Figure 7. Impact on the polarization curve of the samples before and after cryogenic treatment; **1**—Before cryogenic treatment; **2**—After cryogenic treatment, −180 °C, 4 h; **3**—After cryogenic treatment, −180 °C, 6 h; **4**—After cryogenic treatment, −180 °C, 8 h.

5. Conclusions

1. After the deep cryogenic treatment, there is no phase change in the AZ61 magnesium alloy welded joints, but the organization of α and β phases are refined. The precipitation of β-phase increases significantly and is distributed uniformly; the difference between the three regions of the joint is decreased.
2. The microstructural changes have a great influence on the corrosion behavior of the AZ61 magnesium alloy welded joints. The microstructural changes in the joints caused by the deep cryogenic treatment are beneficial to improve the corrosion resistance of the whole joint.

Author Contributions: Zhisheng Wu and Xiaoyuan Gong conceived and designed the experiments; Xiaoyuan Gong performed the experiments and analyzed the data; Fei Zhao contributed materials and analysis tools; Xiaoyuan Gong wrote the paper.

Conflicts of Interest: All three authors claim that there is no conflict of interest.

References

1. Zhang, W.; Bai, P.; Yang, J.; Xu, H.; Dang, J.; Du, Z. Tensile behavior of 3104 aluminum alloy processed by homogenization and cryogenic treatment. *Trans. Nonferrous Met. Soc. China.* **2014**, *24*, 2453–2458. [CrossRef]
2. Niaki, K.S.; Vahdat, S.E. Fatigue Scatter of 1.2542 Tool Steel after Deep Cryogenic Treatment. *Mater. Today Proc.* **2015**, *2*, 1210–1215. [CrossRef]
3. Amini, K.; Akhbarizadeh, A.; Javadpour, S. Investigating the effect of quench environment and deep cryogenic treatment on the wear behavior of AZ91. *Mater. Des.* **2014**, *54*, 154–160. [CrossRef]

4. Idayan, A.; Gnanavelbabu, A.; Rajkumar, K. Influence of Deep Cryogenic Treatment on the Mechanical Properties of AISI 440C Bearing Steel. *Proced. Eng.* **2014**, *97*, 1683–1691. [CrossRef]
5. IShak, M.; Yamasaki, K.; Maekawa, K. Microstructure and Corrosion Behavior of Laser Welded Magnesium Alloys with Silver Nanoparticles. *World Acad. Sci., Eng. Technol.* **2010**, *70*, 354–359.
6. Cao, F.; Song, G.-L.; Atrens, A. Corrosion and passivation of magnesium alloys. *Corros. Sci.* **2016**, *111*, 835–845. [CrossRef]
7. Mónica, P.; Bravo, P.M.; Cárdenas, D. Deep cryogenic treatment of HPDC AZ91 magnesium alloys prior to aging and its influence on alloy microstructure and mechanical properties. *J. Mater. Proc. Technol.* **2017**, *239*, 297–302. [CrossRef]
8. Pu, Z.; Dillon, O.W., Jr.; Puelo, D.A.; Jawahir, I.S. Cryogenic machining and burnishing of magnesium alloys to improve in vivo corrosion resistance. *Surf. Modif. Magnes. Alloy. Biomed. Appl.* **2015**, *2*, 103–133.
9. Templemana, Y.; Hamub, G.B.; Meshia, L. Friction stir welded AM50 and AZ31 Mg alloys: Microstructural evolution and improved corrosion resistance. *Mater. Charact.* **2017**, *126*, 86–95. [CrossRef]
10. Liao, J.; Hotta, M. Corrosion products of field-exposed Mg-Al series magnesium alloys. *Corros. Sci.* **2016**, *112*, 276–288. [CrossRef]